SCIPEDIA

# Research on Master Production Schedule Optimization of Fast-Moving Consumer Goods Companies Based on the APO-NSAGA Algorithm

Fanghua Ning*, Yutao Jin, Panlong Zhang and Xiangyu Yang

School of Mechanical Engineering, Zhejiang Sci-Tech University, Hangzhou, 310018, China


**INFORMATION**

**Keywords:**
Fast-moving consumer goods
master production schedule
multi-objective optimization
artificial protozoa optimizer
genetic algorithm

**DOI:** 10.23967/j.rimni.2024.10.56426

Revista Internacional de Métodos Numéricos para Cálculo y Diseño en Ingeniería

# Research on Master Production Schedule Optimization of Fast-Moving Consumer Goods Companies Based on the APO-NSAGA Algorithm

**Fanghua Ning***, **Yutao Jin, Panlong Zhang and Xiangyu Yang**

School of Mechanical Engineering, Zhejiang Sci-Tech University, Hangzhou, 310018, China

**ABSTRACT**

This study addresses several issues related to the Master Production Schedule (MPS) in companies, such as over-reliance on manual scheduling by planners, failure to consider the overall perspective of the company, lack of consideration for the impact of seasonal demand fluctuations on the MPS, overlooking potential losses due to stockouts and the resulting loss of market share, inability to adjust the MPS in a timely manner to respond to complex and rapidly changing market demands, and the suboptimal outcomes of the manually compiled production plans. To address these problems, an MPS model is established with the goals of optimizing equipment utilization balance, production costs, inventory costs, and delay costs while comprehensively considering the annual product demand. Subsequently, the artificial protozoan optimization non-dominated sorting adaptive genetic algorithm (APO-NSAGA) is developed based on the artificial protozoan optimization (APO) and the non-dominated sorting genetic algorithm (NSGA-II). In this algorithm, autotrophic, heterotrophic, and dormancy behaviors are used to enhance the local search capability and guide the algorithm's evolutionary process. A self-adaptive crossover and mutation operator, which adjusts according to the number of iterations, is designed to allow the algorithm to converge faster in the early stages of operation and better preserve population diversity and high-fitness individuals in the later stages, thus improving algorithm performance. Finally, through simulation examples, an analysis is conducted on the monthly production volume of the company's three major product categories, as well as the monthly production, available sales, and demand quantities, end-of-month inventory, stock-to-sales ratio, and inventory turnover rate of five typical products. The results demonstrate that the MPS obtained using the proposed model and algorithm achieves comprehensive optimization.

OPEN ACCESS

**Received:** 22/07/2024

**Accepted:** 01/11/2024

**Published:** 07/04/2025

**DOI**
10.23967/j.rimni.2024.10.56426

**Keywords:**
Fast-moving consumer goods
master production schedule
multi-objective optimization
artificial protozoa optimizer
genetic algorithm

*Correspondence: Fanghua Ning (m13586299720@163.com). 

## 1 Introduction

Fast-Moving Consumer Goods (FMCG) are an essential part of daily life and can bring stable and considerable profits to companies [1]. FMCG has the characteristics of a short consumption cycle, numerous similar products, and a high degree of product homogeneity, which also leads to low consumer loyalty. The uncertainty in demand impacts FMCG companies more severely than in other manufacturing industries, especially the Master Production Schedule (MPS) [2]. MPS is a critical activity for the success of manufacturing companies, as the fundamental performance of any production system depends on the proper planning of the MPS. According to the Association for Operations Management (APICS), the MPS is a statement of what the company expects to produce, driving a series of plans, such as material requirements planning. It represents the configuration, quantity, and specific dates of the products the company intends to manufacture. The MPS is not a sales forecast but a statement of demand that needs to account for various factors, such as demand, open orders, material supply, projected ending inventory levels, capacity availability, management policies, and objectives. It provides information on the company's expected inventory balance, available-to-promise quantity, and available capacity. Therefore, FMCG companies need a more precise and agile MPS. However, most FMCG companies still rely on planners to manually prepare the MPS, lacking automation in MPS preparation. In the face of a complex and volatile market environment, the manually prepared MPS often fail to match complex and changeable actual demand in time. When preparing the MPS, companies typically consider only the market demand for the current or next two months without a comprehensive consideration of the annual perspective. This results in severe waste of production resources, low order delivery rates during peak demand months, and high inventory levels. In order to solve these issues, many scholars have conducted research.

(1) Production plan optimization and inventory optimization

For production planning optimization and inventory optimization problem, Framinan et al. [3] constructed a Mixed-Integer Linear Programming (MILP) model, which is capable of reasonably allocating existing inventory and preparing for potential future orders. To analyze the model's performance, they also conducted computational simulations using a testing platform that covers a wide range of business scenarios. Peng et al. [4] considered uncertainty factors, adopting fuzzy programming methods to establish a fuzzy model, which balanced and optimized the objective function under uncertain environments. Wang et al. [5] reconstructed the deterministic model into an uncertain model and constructed two moment-based robust models based on the characteristics of the uncertain models. The experimental results show that the example variant model can deal with the uncertainty problem better, and the second moment model has better performance than the first moment model. Li et al. [6] integrated strategic capacity planning, aggregate planning, master scheduling, and material requirements planning, achieving multi-objective, comprehensive optimal production planning and scheduling. Liu et al. [7] aimed to minimize conversion costs, conversion times, production costs, and inventory costs between different products on the production line, establishing a dynamic model for multi-variety product production planning under multiple uncertainties. Jing et al. [8] constructed a multi-objective collaborative production planning model for distributed systems composed of multiple factories, with the goal of maximizing overall benefits and minimizing individual benefit deviations. Masruroh et al. [9] analyzed a three-tier supply chain network, constructed a multi-period production planning model, and proved that the model effectively copes with uncertainty and reduces total production costs. Yazd et al. [10] constructed a dual-objective integer mathematical model considering load constraints. Through this model, they obtained the optimal production plan. Razm et al. [11] constructed a discrete-time production planning model for the characteristics of biorefineries, providing effective guidance for their production. Marfuah et al. [12] used dynamic programming to construct an aggregate production planning (APP) model under uncertainty, proving its low error value through simulation. Bazo do Nascimento et al. [13] studied the production scheduling problem of open workshops, built a mathematical model with workers' flexibility and no waiting as optimization goals and workers' skills as constraints, and proved the effectiveness of this model through several production benchmarks.

(2) Optimization algorithms

In terms of production plan optimization algorithms, Deng et al. [14] designed an improved particle swarm optimization (PSO). This algorithm adjusts the convergence weights of particles in both global and local optimization by incorporating nonlinear dynamic inertia weights and dynamically corrected penalty factors. It is capable of adapting to the characteristics of multi-period iterations and exhibits good convergence performance. Chaudhry et al. [15] designed an easy-to-use genetic algorithm framework using Microsoft Excel spreadsheets. After comparative analysis, the genetic algorithm designed by them can solve the benchmark problem efficiently and effectively and has a certain precision. Ferreira et al. [16] designed the clarke and wright's savings, tabu search and non-dominated sorting genetic algorithm-II (CWNSGA-II) and the clarke and wright's savings with the non-dominated sorting genetic algorithm-II (CWTSNSGA-II), and proved the excellent performance of these two algorithms by comparing them with the non-dominated sorting genetic algorithm (NSGA-II) and the multi-objective particle swarm optimization algorithm (MOPSO). Wang et al. [17] proposed a heuristic algorithm, aggregation particle swarm optimization and a self-adaptive genetic operator (APSO-SGO), which combines PSO and adaptive genetic operator (SGO) based on population aggregation degree. The algorithm can adjust the adaptive crossover and mutation operators according to the state and mass of particles to achieve a dynamic balance between global and local search capabilities. Guzman et al. [18] proposed a method combining genetic algorithms and mixed-integer linear programming models, testing the algorithm using the Coin-OR branch and cut open-source solver and proving its reliability. Bojic et al. [19] combined genetic algorithms with discrete event simulation, testing the results through a simulation model and demonstrating the superiority and efficiency of genetic algorithms in production plan optimization. Lin et al. [20] proposed a comprehensive optimization algorithm (DNNA-GAVOA) that combines the deep neural network acceleration-double-layer optimization method (DNNA-DOM) and African vulture optimization algorithm (AVOA), and they also proved the algorithm's excellent optimization stability. Wang et al. [21] designed a novel metaheuristic algorithm—the black kite algorithm (BKA), which integrates the Cauchy mutation strategy and Leader strategy, enhancing the algorithm's global search ability and convergence speed. It achieves a good balance between exploring global solutions and exploiting local information. Wang et al. [22] proposed a metaheuristic algorithm based on the survival and predation behaviors of the Atlantic Puffin. This algorithm is divided into an exploration phase and an exploitation phase. In the exploration phase, the introduction of the Levy flight factor and speed factor enhances the algorithm's ability to jump out of the local optimal solution, while in the exploitation phase, strategies such as cooperative and adaptive variation factors ensure the global search capability of the algorithm. They also validated the superior performance of the algorithm through test sets and real-world engineering problems. Wang et al. [23] designed a new artificial protozoa optimizer (APO) by simulating the foraging, dormancy, and reproduction mechanisms of protozoa. The algorithm's superior performance was validated through experimental simulations, comparison with 32 advanced algorithms, the Wilcoxon signed-rank test, and the Friedman test.

In summary, scholars have conducted extensive research on optimization models for production planning, such as multi-level production planning and scheduling integration models, fuzzy optimization models based on fuzzy programming methods, dynamic production planning models under multiple uncertainties, multi-objective collaborative production planning models, multi-period production planning models, and multi-objective optimization models. These optimization models, while considering market demand uncertainty, achieve optimization and improvement of enterprise production plans by mathematically describing the production processes. Regarding optimization algorithms, the combination of intelligent optimization algorithms such as genetic algorithms, particle swarm optimization, black kite optimization, and Atlantic Puffin optimization, along with the introduction of some innovative techniques, has effectively enhanced the performance and optimization effectiveness of these algorithms. However, most existing research focuses on specific issues such as production planning and scheduling, with little consideration from the perspective of the overall enterprise for MPS. When planning the MPS, seasonal peaks and troughs in product demand are often overlooked, resulting in a less reasonable MPS. Additionally, most studies only consider the direct losses caused by product stockouts when evaluating stockout-related losses, neglecting potential losses such as market share loss due to stockouts. To better address these issues, this paper takes a comprehensive view of fast-moving consumer goods enterprises. When constructing the MPS model, the product market share loss formula is introduced, taking potential losses caused by stockouts into account as one of the objective functions. The data basis for calculating product demand constraints is extended from three months to a full year to fully account for the impact of product demand during peak and off-peak seasons, making the MPS more precise and reasonable. Furthermore, the genetic algorithm (GA) is an optimization algorithm based on the theory of biological evolution. Its core idea is to simulate the processes of genetic inheritance, crossover, and mutation to achieve the optimal solution to the optimization problem. GA has a wide range of applications, strong global search ability, simplicity in operation, and scalability. The APO, on the other hand, simulates the behavior patterns of protozoa in nature, such as foraging, heterotrophy, dormancy, and reproduction, to solve problems. APO has strong local search ability and is effective in solving continuous problems. Given that the formulation and optimization of the master production schedule is a discrete problem, this paper proposes the artificial protozoan optimization non-dominated sorting adaptive genetic algorithm (APO-NSAGA), which is designed based on the GA and APO. The algorithm leverages the excellent scalability of GA, combining it with APO by simplifying APO's complex operations through GA, improving APO's adaptability to discrete problems. Meanwhile, APO's excellent local search ability compensates for the local search weakness of GA.

This paper is divided into three parts. The first part constructs an optimized MPS model based on the actual needs of fast-moving consumer goods enterprises, with objectives such as balancing equipment usage, minimizing production costs, minimizing inventory costs, and minimizing delay costs. The second part designs the APO-NSAGA based on the NSGA-II and the APO and verifies the performance of this algorithm. The third part takes Company A in the cigarette industry as a case study, selecting 16 products and 39 production machines for calculation and conducting an in-depth analysis of five typical products.

## 2 Multi-Objective Master Production Planning Optimization Model

### *2.1 Objective Functions*

The MPS is a plan that an enterprise formulates based on product market demand, combining sales forecast plans with its actual production capacity. It involves pre-arrangements regarding product types, production time, production priority, production volume, the allocation of human and equipment resources, and inventory management. The MPS reflects the various indicators, production progress, and corresponding environmental adjustments that the enterprise should achieve within a planning period [24,25]. For industry, the ultimate goal of developing the MPS is to better meet market demands. A reasonable MPS can balance the utilization rate of production resources, reduce production costs, inventory costs, and other expenditures while satisfying market demand [26]. Therefore, according to the principles of balanced scheduling and the overall goal of profit maximization, the objective functions are designed as shown in Eqs. (1)–(4). Table 1 shows the all the variables in the master production planning optimization model.

**Table 1:** The variables in the master production planning optimization model

| Serial number | Variable | Annotation |
|---|---|---|
| 1 | $j$ | The equipment number. |
| 2 | $m$ | The total number of pieces of equipment. |
| 3 | $x_i$ | The planned output of product $i$. |
| 4 | $my_j$ | The 0–1 variable, which represents the usage status of production equipment. |
| 5 | $nd_j$ | The normal production days of equipment $j$. |
| 6 | $od_j$ | The overtime days of equipment $j$. |
| 7 | $\overline{nd}$ | The average normal production days of equipment. |
| 8 | $\overline{od}$ | The average overtime production days of equipment. |
| 9 | $n$ | The total number of product kinds. |
| 10 | $ot_{ij}$ | The overtime production cost of equipment $j$ used to produce product $i$. |
| 11 | $odd_{ij}$ | The overtime production days of the equipment $j$ used to produce product $i$. |
| 12 | $eec_{ij}$ | The energy cost of equipment $j$ used to produce product $i$. |
|  | $ndd_{ij}$ | He normal production days of the equipment $j$ used to produce product $i$. |
| 13 | $chn_i$ | The number of line changes for product $i$. |
| 14 | $scoc_i$ | The additional cost incurred per line change for product $i$. |
| 15 | $inl_i$ | The inventory level of product $i$. |
| 16 | $sinc_i$ | The unit inventory cost of product $i$. |
| 17 | $ind_i$ | The inventory days of product $i$. |
| 18 | $lx_i$ | The quantity of product $i$ that is backordered. |
| 19 | $sedc_i$ | The cost of delaying delivery by one day for an unit product $i$. |
| 20 | $d_i$ | The backorder days of product $i$. |
| 21 | $s_i$ | The current market share of product $i$. |
| 22 | $r$ | The number of out-of-stock occurrences within this production period for every product. |
| 23 | $h_i$ | The consumer retention coefficient after the product $i$ returns to normal supply, usually 0.95 but can be adjusted based on actual conditions. |
| 24 | $kd_v$ | The correction coefficients for product $v$ ($v = 1, 2, 3, 4$) categories. |
| 25 | $\rho_i$ | The lagged supply rate. |
| 26 | $\tau_i$ | The waiting time for consumers to purchase product $i$. |
| 27 | $k_{i0}$ | The out-of-stock lag sensitivity factor for product $i$. |
| 28 | $k_{i1}$ | The waiting time sensitivity factor for product $i$. |
| 29 | $l$ | The sales region of every product. |
| 30 | $L$ | The total number of sales regions for every product. |
| 31 | $tpe_i$ | The total customer base for product $i$. |
| 32 | $pe_{il}$ | The customer base for product $i$ in region $l$. |

(Continued)

**Table 1 (continued)**

| Serial number | Variable | Annotation |
|---|---|---|
| 33 | $tsa_i$ | The total sales of product. |
| 34 | $sa_{il}$ | The total sales of product $i$ in region $l$. |
| 35 | $sft_{il}$ | The market satisfaction for product $i$ in region $l$. |
| 36 | $dem_i$ | The market demand for product $i$ within this production planning period. |
| 37 | $A$ | The total market demand within this production planning period. |
| 38 | $\beta$ | The market demand fluctuation coefficient. |
| 39 | $AP_i$ | The market demand for product $i$ within this production planning period. |
| 40 | $d_i^{\pm}$ | The demand correction coefficient for product $i$. |
| 41 | $AM_i^{mon-1}$ | The market demand for product $i$ in the next production planning period. |
| 42 | $mon$ | The current production planning period. |
| 43 | $b_{mon-1}$ | The adjustment coefficient. |
| 44 | $q$ | The last production planning period. |
| 45 | $R$ | The maximum ratio of overtime days to normal working days within this planning period. |
| 46 | $OW$ | The maximum normal working days within this production planning period. |
| 47 | $NW$ | The maximum overtime days within this production planning period. |
| 48 | $umac_i$ | The number of equipment actually used to produce product $i$. |
| 49 | $kmac_i$ | The total number of equipment that can produce product $i$. |
| 50 | $pr_{ij}$ | The daily output of equipment $j$ used to produce product $i$. |
| 51 | $mac$ | The number of production equipment actually used within this production planning period. |
| 52 | $INC$ | The inventory level upper limit. |

(1) Balancing equipment usage

When arranging production, enterprise need to balance the usage of equipment as much as possible. Eq. (1) measures the load status of the equipment, aiming to make the usage of equipment more plausible:

$$Min\left(f_1\right) = \frac{\sum_j^m my_j * \left(nd_j - \overline{nd}\right)^2}{m} + \upsilon * \frac{\sum_j^m my_j * \left(od_j - \overline{od}\right)^2}{m} \tag{1}$$

where $j$ is the equipment number. $m$ is the total number of pieces of equipment. $x_i$ is the planned output of product $i$. $my_j$ is the 0–1 variable, which represents the usage status of production equipment. If equipment $j$ is actually put into use, its value is 1, otherwise it is 0. $nd_j$ are the normal production days of equipment $j$. Normal production refers to the production activities carried out by the enterprise on legal working days. $od_j$ are the overtime production days of equipment $j$. Overtime production refers to production activities outside normal production hours. $\overline{nd}$ are the average normal production days of equipment. $\overline{od}$ are the average overtime production days of equipment.

(2) Minimizing production costs

Production costs include regular production costs, overtime costs, and additional costs incurred by production line changes. For make-to-order enterprises, regular costs can be regarded as fixed values. Eq. (2) aims to minimize production costs:

$$Minx\,(f_2) = \sum_{i=1}^{n}\sum_{j=1}^{m}\left(ot_{ij} * odd_{ij} * my_j\right) + \sum_{i=1}^{n}\sum_{j=1}^{ma_i} eec_{iz} * \left(nd_{ij} + odd_{ij} * my_j\right) + \sum_{i=1}^{n} chn_i * scoc_i \tag{2}$$

where $n$ is the total number of product kinds. $ot_{iz}$ is the overtime production cost of equipment $z$ used to produce product $i$. $odd_{ij}$ are the overtime production days of the equipment $j$ used to produce product $i$. $eec_{ij}$ is the energy cost of equipment $j$ used to produce product $i$. $ndd_{ij}$ are the normal production days of the equipment $j$ used to produce product $i$. Raw material costs and normal working costs in the production process can be regarded as fixed values, so they are not considered. In addition, FMCG is typically produced on assembly lines. When changing the type of product produced on a production line, the equipment on the entire line needs to be adjusted, and processes such as material withdrawal, cleaning, label changing, and inspection must be performed before the line can be used to produce a different product. This process inevitably incurs additional costs, referred to as changeover costs. Therefore, introduce the following variables. $chn_i$ is the number of line changes for product $i$. $scoc_i$ is the additional cost incurred per line change for product $i$.

(3) Minimizing inventory costs

In actual production management, finished goods inventory management is an important part of controlling cost expenditures. Eq. (3) aims to minimize the inventory cost by controlling the product inventory quantity, thereby reducing the enterprise's inventory cost:

$$Min\,(f_3) = \sum_{i=1}^{n} inl_i * sinc_i * ind_i \tag{3}$$

where $inl_i$ is the inventory level of product $i$. $sinc_i$ is the unit inventory cost of product $i$. $ind_i$ are the inventory days of product $i$.

(4) Minimizing backorder cost

Eq. (4) aims to minimize the delay cost. Delay cost refers to the losses incurred when a company is unable to deliver products on time or in the agreed quantity. These losses can be divided into two categories: direct and indirect losses. Direct losses include penalties for breaching delivery agreements and reduced company revenue due to delayed deliveries. Indirect losses refer to the product shortages in the market caused by the company's inability to deliver on time, leading to the loss of potential customers and potential market share [26]:

$$Min\,(f_4) = \sum_{i=1}^{n} lx_i * sdec_i * d_i + \sum_{i=1}^{n} kd_v(1 - h_i^r(1 - \rho_i)) * s_i \tag{4}$$

where $lx_i$ is the quantity of product $i$ that is backordered. $sedc_i$ is the cost of delaying delivery by one day for a unit product $i$. $d_i$ is the backorder days of product $i$. $s_i$ is the current market share of product $i$. $r$ is the number of out-of-stock occurrences within this production period for every product. $h_i$ is the consumer retention coefficient after the product $i$ returns to normal supply, usually 0.95 but can be adjusted based on actual conditions. $kd_v$ are the correction coefficients for product $v$ ($v = 1, 2, 3, 4$) categories. $kd_1$ is the correction coefficient for star products, the number usually is 1.4. $kd_2$ is the correction coefficient for cash cow products, the number usually is 1.2. $kd_3$ is the correction coefficient for problem products, the number usually is 0.9. $kd_4$ is the correction coefficient for dog products, the number usually is 0.7. $\rho_i$ is the lagged supply rate, indicating the willingness of consumers to wait for lagged supply influenced by the length of waiting time.

(1) Lagged supply rate $\rho_i$

Eq. (5) is the improved formula for calculating the lagged supply rate, used to measure the market share loss caused by out-of-stock situations:

$$\rho_i = \frac{k_{i0}}{1 + k_{i1}\tau_i} \tag{5}$$

where $\tau_i$ is the waiting time for consumers to purchase product $i$. $k_{i0}$ is the out-of-stock lag sensitivity factor for product $i$. $k_{i1}$ is the waiting time sensitivity factor for product $i$.

(2) Out-of-stock lag sensitivity factor $k_{i0}$ and waiting time sensitivity factor $k_{i1}$

The calculation process of $kor_{i0}$ is shown in the following equation. $kor_{i0}$ is a transition variable, no practical significance:

$$kor_{i0} = \sum_{l}^{L} \left( sft_{il} * \frac{pe_{il}}{tpe_i} * \frac{sa_{il}}{tsa_i} \right) \tag{6}$$

where $l$ is the sales region of every product. $L$ is the total number of sales regions for every product. $tpe_i$ is the total customer base for product $i$. $pe_{il}$ is the customer base for product $i$ in region $l$. $tsa_i$ are the total sales of product. $sa_{il}$ are the total sales of product $i$ in region $l$. $sft_{il}$ is the market satisfaction for product $i$ in region $l$.

Eq. (7) standardizes the results of Eq. (6), making the out-of-stock lag sensitivity factor value range between 0–1.

$$k_{i0} = \frac{kor_{i0} - Min\,(kor_{i0})}{Max\,(kor_{i0}) - Min\,(kor_{i0})},\ (0 < k_{i0} < 1) \tag{7}$$

The calculation process of $k_{i1}$ is shown in Eq. (8):

$$k_{i1} = \ln\,(dem_i - x_i)\,,\ (k_{i1} > 0) \tag{8}$$

where $dem_i$ is the market demand for product $i$ within this production planning period.

### *2.2 Constraints*

After determining the objective functions, the constraints of the model need to be designed according to various factors and limitations that need to be considered in the formulation of the MPS and the actual production process to ensure that the constructed MPS model conforms to reality. By thoroughly understanding and analyzing the MPS formulation process and actual production process of manufacturing enterprises, the constraints of the model are determined, as shown in Eqs. (9)–(16).

Eq. (10) considers the constraint on total output under the premise of demand uncertainty:

$$\sum_{i}^{n}(x_i + inl_i) \geq \beta * A \tag{9}$$

where $A$ is the total market demand within this production planning period. $\beta$ is the market demand fluctuation coefficient, which is used to reduce the impact of market demand uncertainty.

Eq. (11) represents the output constraint for each product category, which considers the impact of demand uncertainty and future demand:

$$x_i + inl_i \geq d_i^{\pm} * (A_{pi} + b_{mon-1} * AM_i^{mon-1} + \ldots + b_{mon-1-q} * AM_i^{mon-1-q}) \tag{10}$$

where $AP_i$ is the market demand for product $i$ within this production planning period. $d_i^{\pm}$ is the demand correction coefficient for product $i$, which is related to market share and sales prospects. $AM_i^{mon-1}$ is the market demand for product $i$ in the next production planning period. $mon$ is the current production planning period. $q$ is the last production planning period.

Eq. (12) represents the constraint on the time of overtime, which means the monthly actual time of overtime must be within the allowable range:

$$\frac{odd_{ij}}{ndd_{ij}} \leq R, \forall odd_{ij} \leq OW, ndd_{ij} \leq NW \tag{11}$$

where $R$ is the maximum ratio of overtime days to normal working days within this planning period. $OW$ is the maximum normal working days within this production planning period. $NW$ is the maximum overtime days within this production planning period.

Eq. (13) represents the constraint on the number of production equipment available for use, which means the number of equipment actually used each month cannot exceed the total number of equipment:

$$umac_i \leq kmac_i \tag{12}$$

where $umac_i$ is the number of equipment actually used to produce product $i$. $kmac_i$ is the total number of equipment that can produce product $i$.

Eq. (14) represents the capacity constraint of the equipment, which means the planned output of each product each month cannot exceed the equipment's capacity limit:

$$x_i \leq \sum_{i=1}^{n} \sum_{j=1}^{m} pr_{ij} * \left(odd_{ij} + ndd_{ij}\right) * my_j \tag{13}$$

where $pr_{ij}$ is the daily output of equipment $j$ used to produce product $i$.

Eq. (15) represents the utilization rate constraint of the equipment, which means the number of equipment actually used each month must be greater than a certain value:

$$1.0 \geq \frac{mac}{m} \geq 0.80 \tag{14}$$

where $mac$ is the number of production equipment actually used within this production planning period.

Eq. (16) represents the inventory level constraint, which means the total inventory each month must be within the allowable range:

$$\sum_{i=1}^{n} inl_i \leq INC \tag{15}$$

where $INC$ is the inventory level upper limit.

Besides, in the same production period, the usage status of each production equipment is unique. This means that at the same time, the value of $my_j$ is unique.

## 3 Design of the Improved APO-NSAGA Algorithm

The core idea of the GA is to convert the problem's solution into chromosomes. By simulating processes such as gene inheritance, crossover, and mutation, GA searches for the optimal solution to the problem [27]. The APO, on the other hand, mimics the behaviors of protozoa in nature, including foraging, heterotrophy, dormancy, and reproduction, to solve problems [23]. The APO compensates for GA's weaknesses, such as poor local search capability and the iterative evolution process lacks clear direction, while GA can address APO's tendency to get trapped in local optima and its high complexity. However, the complete mathematical process for these techniques needs to be defined based on the specific problem, without any strict predefined mathematical theory, precise mathematical relationships, or related laws [28]. Therefore, based on the above analysis and the multi-objective master production schedule optimization model, NSGA-II and APO algorithm are selected for integration. NSGA-II is a type of genetic algorithm that effectively addresses multi-objective optimization problems. Compared to the traditional GA algorithm and non-dominated sorting genetic algorithm (NSGA), NSGA-II is used to solve multi-objective optimization problems and resolves the issue of high time complexity in traditional nondominated sorting methods by using a fast nondominated sorting approach. This ensures population diversity, effectively reduces the computational load of the algorithm, and significantly improves its execution speed. The process of the APO-NSGA designed in this paper is shown in Fig. 1. Table 2 shows all the variables in the APO-NSAGA.

### *3.1 Chromosome Code and Fitness Function Design*

#### *3.1.1 Chromosome Code*

In NSGA-II, each solution to the problem is represented as an individual, and each individual is composed of chromosomes. The fitness of an individual reflects how well the solution fits the problem. The algorithm determines the suitability of a solution by calculating the fitness of the individual. Therefore, before designing the algorithm, the solution must be converted into chromosomes to form individuals. The encoding process is based on predetermined encoding rules that map the solution space of the problem to the corresponding encoding space, thereby transforming the solution into chromosomes and forming corresponding individuals. The quality of the encoding directly affects the solution accuracy and efficiency of the algorithm. Common encoding methods include integer encoding, floating-point encoding, and binary encoding. Considering that the variables in the master production schedule optimization problem are all non-negative integers, integer encoding is adopted.

According to the constructed multi-objective master production schedule optimization model, each individual is composed of at most 12 chromosomes and at least 1 chromosome, with the specific number depending on the current month. For example, if a company sets February as the starting month of the annual production and January of the following year as the end month, and the current month is July, then each individual in the algorithm consists of 7 chromosomes, corresponding to the master production schedule for 7 months. The master production schedule for the current month is the most accurate and can be used for actual production, while the schedules for the following months are forecast plans that need to be continuously updated and adjusted based on actual demand changes.

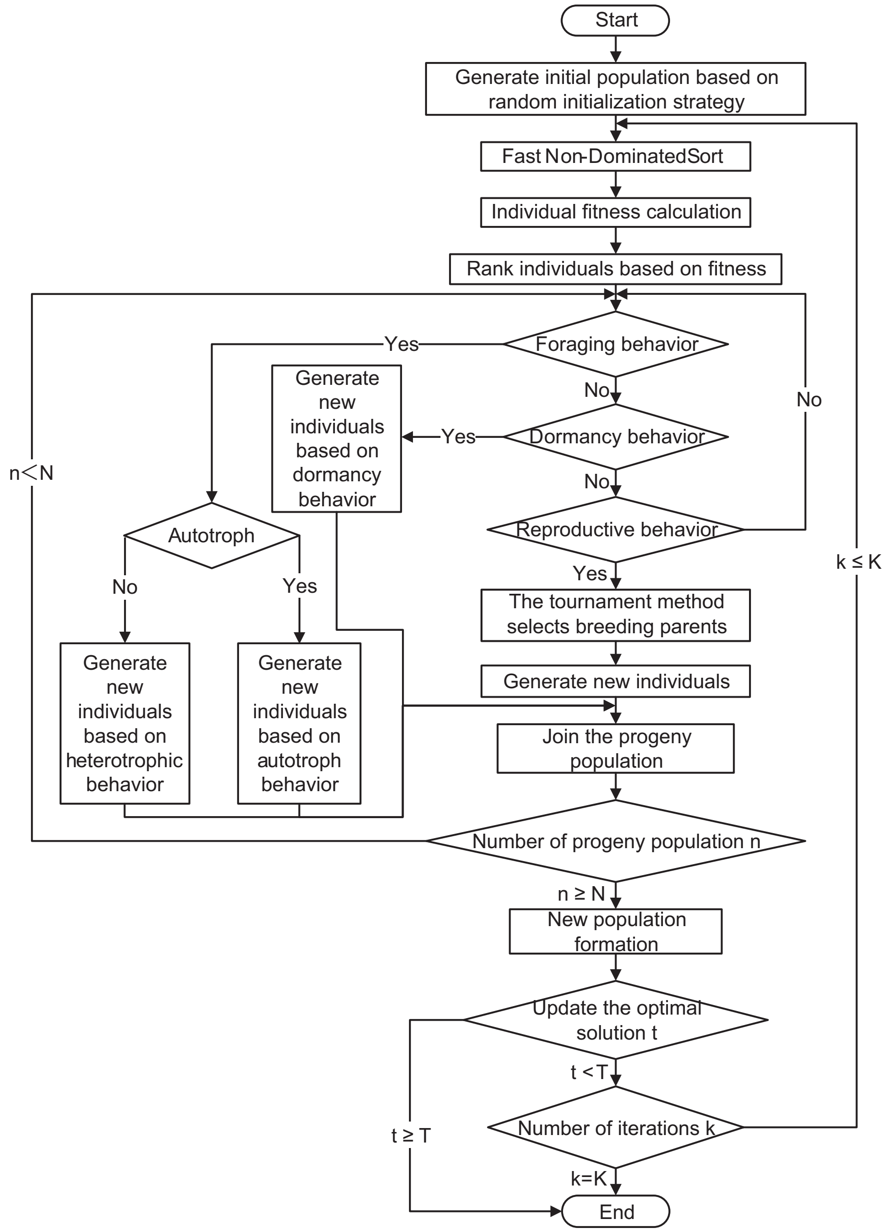


**Figure 1:** Flowchart of APO-NSAGA

**Table 2:** The variables in the APO-NSAGA

| Serial number | Variable | Annotation |
|---|---|---|
| 1 | $xp_i$ | The individual $i$. |
| 2 | $o_1, o_2, o_3$ | The correction coefficient value, and the values are 1.4, 1.2, and 1.4, respectively. |

(Continued)

**Table 2 (continued)**

| Serial number | Variable | Annotation |
|---|---|---|
| 3 | $p_{ah}$ | The probability of individuals engaging autotrophic and heterotrophic behaviors. |
| 4 | $gen$ | The current number of iterations of the algorithm. |
| 5 | $maxgen$ | The maximum number of iterations. |
| 6 | $ac$ | The 0–1 variable, which is used to judge the specific behavior pattern taken by the individual. |
| 7 | $xp_i^{dim}$ | The *dim*-dimensional element of individual $i$. |
| 8 | $ps$ | The population size. |
| 9 | $f$ | The foraging factor. |
| 10 | $np$ | The domain logarithm. |
| 11 | $w_a$ | The weight factor of protozoa engaged in autotrophic behavior. |
| 12 | $xp_{i-k}$ | The previous protozoa adjacent to protozoa $i$ (if $i = 1$, $i - k = i = 1$). |
| 13 | $xp_{i+k}$ | The latter protozoa adjacent to protozoa $i$ (if $i = ps$, $i + k = i = ps$). |
| 14 | $eps$ | A very small positive value ($2.2204^{-16}$). |
| 15 | $M_f$ | The execution vector of autotrophic behavior. |
| 16 | $di$ | The dimensional index. |
| 17 | $xp_i^{new}$ | The individual $i$ that moves to a new location. |
| 18 | $xp_j$ | The individual $j$ which is selected randomly. |
| 19 | $Rand$ | The random vector in which the value of each element is in an [0, 1] interval. |
| 20 | $\pm$ | The direction of movement of protozoa foraging. |
| 21 | $w_h$ | The weight factor of protozoa engaging heterotrophic behavior. |
| 22 | $p_{dr}$ | The probability of an individual engaging dormancy and reproductive behavior. |
| 23 | $pf$ | The proportion of dormant to breeding individuals in a population. |
| 24 | $xp_{min}$ | The protozoa that has minimum fitness. |
| 25 | $lb_{dim}$ | The element of the *dim*-dimension of this protozoa. |
| 26 | $xp_{max}$ | The protozoa that has maximum fitness. |
| 27 | $ub_{dim}$ | The element of the *dim*-dimension of this protozoa. |
| 28 | $P_{ci}$ | The crossover probability of individual $i$. |
| 29 | $P_{mi}$ | The mutation probability of individual $i$. |
| 30 | $P_{c0}$ | The initial values of cross probability. |
| 31 | $P_{m0}$ | The initial values of cross variation probability. |
| 32 | $\alpha_1, \alpha_2, \beta_1, \beta_2$ | The correction factor, their values are 0.9, 1.4, 1.2, and 0.7, respectively. |
| 33 | $\mu$ | The difference between maximum fitness and minimum fitness. |
| 34 | $\gamma$ | A constant value used to judge the convergence of the algorithm. |

Fig. 2 shows the specific structure of the chromosomes in the algorithm. Each chromosome consists of six genes: product type, production month, workdays, overtime, number of equipment, and production priority.

| type | 1 | 2 | 3 | 4 | 5 | 6 | 7 | 8 | 9 | 10 | 11 | 12 | 13 | 14 | 15 | 16 |
|---|---|---|---|---|---|---|---|---|---|---|---|---|---|---|---|---|
| month | 7 | 7 | 7 | 7 | 7 | 7 | 7 | 7 | 7 | 7 | 7 | 7 | 7 | 7 | 7 | 7 |
| workday | 46 | 65 | 41 | 83 | 12 | 93 | 12 | 0 | 0 | 0 | 74 | 97 | 83 | 32 | 21 | 9 |
| overtime | 0 | 4 | 9 | 13 | 4 | 4 | 0 | 0 | 0 | 0 | 6 | 5 | 3 | 0 | 21 | 0 |
| number of equipment | 15 | 15 | 13 | 10 | 10 | 10 | 15 | 15 | 13 | 15 | 15 | 13 | 15 | 13 | 13 | 15 |
| Production priority | 13 | 1 | 2 | 5 | 15 | 11 | 9 | 7 | 6 | 14 | 16 | 8 | 12 | 3 | 10 | 4 |

**Figure 2:** Chromosome structure

After the calculation is completed, it is also necessary to restore the solution represented by each individual in the algorithm, which is decoding. Decoding is the inverse process of encoding, that is, the process of mapping the encoding space back to the solution space of the problem. Because of the integer encoding method, no additional decoding operation is required. In addition, this paper generates the initial population based on the random strategy, which is simple to operate and can effectively ensure the diversity and uniformity of the initial population.

#### *3.1.2 Fitness Function Design*

The fitness function evaluates the quality of individuals during the algorithm's process and is closely related to the objective functions of the model. For NSGA-II, it is not necessary to design a separate fitness function. It uses a fast nondominated sorting method to generate a Pareto front based on the four objective functions of the master production schedule optimization model, handling the dominance relationships between individuals. It then ranks individuals within the same Pareto front using crowding distance to ensure population diversity. However, for the convenience of subsequent calculations, the four designed objective functions are aggregated to obtain the fitness function as shown in Eq. (16). This function does not participate in the division of the Pareto front or the calculation of crowding distance, nor does it affect the ranking or selection of individuals. It is only involved in part of the formula calculations.

$$F(x_i) = 6 - \left( \frac{f_1(xp_i) - \min(f_1)}{\max(f_1) - \min(f_1)} + o_1 * \frac{f_2(xp_i) - \min(f_2)}{\max(f_2) - \min(f_2)} + o_2 * \frac{f_1(xp_4) - \min(f_4)}{\max(f_4) - \min(f_4)} \right.$$
$$\left. + o_3 * \frac{f_1(xp_4) - \min(f_4)}{\max(f_4) - \min(f_4)} \right) \tag{16}$$

where $xp_i$ is the individual $i$. $o_1$, $o_2$, $o_3$ is the correction coefficient value, and the values are 1.4, 1.2, and 1.4, respectively.

### ***3.2 Individual Behavior***

After completing the division of the Pareto front and ranking individuals within the same front using the fast nondominated sorting method, it is necessary to design the behavior of the individuals. In addition to the traditional crossover and mutation operations, APO-NSAGA introduces certain individual behavior methods from the APO. These methods are derived from the behaviors protozoa adopt to cope with environmental changes and are described as follows:

(1) Autotrophic behavior: Most protozoa contain chloroplasts and can perform photosynthesis. They autonomously escape areas with excessively high or low light intensity and stay in places with optimal light conditions.

Heterotrophic behavior: When the energy needs of protozoa cannot be met by photosynthesis, they autonomously move toward areas that are rich in food.

(2) Dormant behavior: When environmental conditions become too harsh, protozoa enter a dormant state to endure unfavorable conditions.

(3) Reproductive behavior: When environmental conditions are favorable and the protozoa meet certain internal conditions, they reproduce to generate new individuals.

### *3.2.1 Autotrophic Behavior and Heterotrophic Behavior*

Both autotrophic and heterotrophic behaviors are types of foraging behaviors in protozoa, influenced by both internal and external factors of the protozoan population. The overall occurrence probability of autotrophic and heterotrophic behaviors is shown in Eq. (17), while Eq. (18) is used to determine whether an individual should adopt autotrophic or heterotrophic behavior.

$$p_{ah} = \frac{1}{2}\left(1 + cos\left(\frac{gen}{maxgen}\cdot\pi\right)\right) \tag{17}$$

$$ac = \begin{cases} 1, \ F\left(xp_i\right) > \overline{F} \\ 0, \ F\left(xp_i\right) < \overline{F} \end{cases} \tag{18}$$

where $p_{ah}$ is the probability of individuals engaging autotrophic and heterotrophic behaviors. $gen$ is the current number of iterations of the algorithm. $maxgen$ is the maximum number of iterations. $ac$ is the variable 0–1, where 1 indicates that the individual adopts autotrophic behavior, and 0 indicates that the individual adopts heterotrophic behavior. $xp_i$ are the protozoa $i$, also known as individual $i$. In the subsequent content, $xp_i$ is uniformly referred to as an individual.

The mathematical description of autotrophic behavior and heterotrophic behavior are shown in Eqs. (19) to (24) and Eqs. (25) to (28) [23].

$$xp_i = \left[xp_i^1, \ xp_i^2, \ldots, \ xp_i^{dim}\right] \tag{19}$$

$$f = rand\cdot\left(1 + \cos\left(\frac{gen}{maxgen}\cdot\pi\right)\right) \tag{20}$$

$$np_{max} = \left\lfloor\frac{ps-1}{2}\right\rfloor \tag{21}$$

$$w_a = e^{-\left|\frac{F\left(xp_{i-k}\right)}{F\left(xp_{i+k}\right)+eps}\right|} \tag{22}$$

$$M_f\left[di\right] = \begin{cases} 1, dim \le i \le \lceil\dfrac{i\cdot dim}{ps}\rceil \\ \qquad 0, \end{cases} \tag{23}$$

$$xp_i^{new} = xp_i + f\cdot\left(xp_j - xp_i + \tfrac{1}{np}\textstyle\sum_{k=1}^{np} w_a\left(xp_{i-k} - xp_{i+k}\right)\right)\odot M_f \tag{24}$$

where $xp_i^{dim}$ is the $dim$-dimensional element of individual $i$. $ps$ is the population size. $f$ is the foraging factor. $np$ is the domain logarithm. $w_a$ is the weight factor of individual engaged in autotrophic behavior. $xp_{i-k}$ is the previous individual adjacent to individual $i$ (if $i = 1, i-k = i = 1$). $xp_{i+k}$ is the latter individual adjacent to individual $i$ (if $i = ps, i+k = i = ps$). $eps$ is a very small positive value ($2.2204^{-16}$). $M_f$ is the execution vector of autotrophic behavior. $di$ is the dimensional index. $xp_i^{new}$ is the individual $i$ that moves to a new location. $xp_j$ is the individual $j$ which is selected randomly.

$$Rand = [rand_1, rand_2, \ldots, rand_{dim}] \tag{25}$$

$$x_{near} = \left(1 \pm Rand\left(1 - \frac{gen}{maxgen}\right)\right) \odot x_i \tag{26}$$

$$w_h = e^{-\left|\frac{F(x_{i-k})}{F(x_{i+k})+eps}\right|} \tag{27}$$

$$x_i^{new} = x_i + f \cdot \left(x_{near} - x_i + \frac{1}{np}\sum_{k=1}^{np} w_h\,(x_{i-k} - x_{i+k})\right) \odot M_f \tag{28}$$

where *Rand* is the random vector in which the value of each element is in an [0, 1] interval. $\pm$ is the direction of movement of individual foraging. $w_h$ is the weight factor of individual engaging heterotrophic behavior.

However, while the aforementioned behavior formulas can effectively address continuous problems, they cannot be directly applied to discrete problems, meaning they cannot be directly used within the APO-NSAGA. Therefore, the following improvements are made to convert the discrete problem into a continuous one:

(1) Based on the specific gene information in the chromosomes of an individual and the corresponding production capacity of the equipment, the product output represented by each chromosome is calculated and stored in a matrix, denoted as *mat*. The matrix *mat* is a $w * u$ matrix, where $w$ is the number of chromosomes constituting an individual (related to the current month) and $u$ is the number of product kinds, which is set to 16 in this paper.

$$mat = \begin{bmatrix} mat_{11} & mat_{12} & \cdots & mat_{1u} \\ mat_{21} & mat_{22} & \cdots & mat_{2u} \\ \vdots & \vdots & \ddots & \vdots \\ mat_{w1} & mat_{w2} & \cdots & mat_{wu} \end{bmatrix} \tag{29}$$

(2) The calculated matrix mat is treated as individual xi, and the above behavior formulas are applied to compute a new matrix, denoted as *nmat*. The structure of matrix *nmat* is the same as that of *mat*.

$$nmat = \begin{bmatrix} nmat_{11} & nmat_{12} & \cdots & nmat_{1u} \\ nmat_{21} & nmat_{22} & \cdots & nmat_{2u} \\ \vdots & \vdots & \ddots & \vdots \\ nmat_{w1} & nmat_{w2} & \cdots & nmat_{wu} \end{bmatrix} \tag{30}$$

(3) Based on the updated product output information contained in matrix *nmat*, the chromosomes are regenerated to achieve individual updates in the algorithm. If it is autotrophic behavior, operations such as gene swapping and mutation are performed on the original chromosome's genes using the output information from matrix *nmat* as the target to generate new individuals. If it is heterotrophic behavior, new individuals are generated based on a random strategy, using the output information from matrix *nmat* as the target.

#### *3.2.2 Dormancy Behavior and Reproductive Behavior*

When environmental conditions are harsh, protozoa may adopt dormancy as a survival strategy to cope with adverse external conditions. In the algorithm, if an individual needs to enter dormancy, it indicates poor fitness and an inability to adapt to the 'environment'. Therefore, when an individual needs to enter dormancy, it is frozen, and a new individual is generated to replace it, thereby improving the population's quality and maintaining a constant population size. This process is mathematically described in Eqs. (31) to (35) [23].

$$p_{dr} = \frac{1}{2}\left(1 + \cos\left(\left(1 - \frac{loc_i}{ps}\right)\cdot \pi\right)\right) \tag{31}$$

where $p_{dr}$ is the probability of an individual engaging dormancy and reproductive behavior. $loc_i$ is the position of individual $i$ in the population after ranking.

Additionally, the proportion of individuals engaging dormancy and reproduction in each generation should be regulated to prevent the population size from continually shrinking due to excessive dormancy or expanding due to excessive reproduction. The specific mathematical description is shown in Eq. (32):

$$pf = pf_{max} \cdot rand \tag{32}$$

where $pf$ is the proportion of dormant to breeding individuals in a population. $rand$ is the random number in the interval (0, 1).

$$x_{min} = [lb_1, lb_2, \ldots, lb_{dim}] \tag{33}$$

$$x_{max} = [ub_1, ub_2, \ldots, ub_{dim}] \tag{34}$$

$$xp_i^{new} = xp_{min} + Rand \odot (xp_{max} - xp_{min}) \tag{35}$$

where $xp_{min}$ is the individual that has minimum fitness, and $lb_{dim}$ is the element of the $dim$-dimension of this individual. $xp_{max}$ is the individual that has maximum fitness, and $ub_{dim}$ is the element of the $dim$-dimension of this individual.

The APO generates new solutions by introducing certain perturbations, but this asexual reproduction method relies too heavily on the design of perturbation parameters, which weakens the algorithm's global optimization capability. Therefore, the reproductive behavior of individuals is implemented using the selection, crossover, and mutation operations from the NSGA-II. In this process, the selection operation does not depend on a fitness function but is instead based on the Pareto front and the individuals' crowding distance, using a binary tournament method for selection.

However, the crossover and mutation operators in NSGA-II are usually fixed values and do not change as the algorithm iterates. In fact, during the early stages of the algorithm, individual differences are large, so a higher crossover probability should be chosen to increase the generation rate of new individuals, and a lower mutation probability should be selected to accelerate the convergence of the algorithm. In the later stages of the algorithm, a lower crossover probability should be used to protect well-adapted individuals, while a higher mutation probability should be employed to increase population diversity. Thus, adaptive strategies, as shown in Eqs. (36)–(39), are proposed to continuously update the values of the crossover probability and mutation probability based on the number of iterations and the fitness of the individuals.

$$P_{ci} = \begin{cases} P_{c0} - \alpha_1 \dfrac{gen}{maxgen} \dfrac{|F(x_i) - F(avg)|}{\max(F(x)) - \min(F(x))}, \ \mu \geq \gamma \\ P_{c0} - \alpha_2 \dfrac{gen}{maxgen}, \ \mu < \gamma \end{cases} \tag{36}$$

$$P_{mi} = \begin{cases} P_{m0} - \beta_2 \dfrac{gen}{maxgen}, \mu \geq \gamma \\ P_{m0} - \beta_1 \dfrac{gen}{maxgen} \dfrac{|F(x_i) - F(avg)|}{\max(F(x)) - \min(F(x))}, \mu \geq \gamma \end{cases} \tag{37}$$

$$\mu = |\max(f(x)) - \min(f(x))| \tag{38}$$

$$\gamma = 1.3 * \left(\max\left(F(x) - \overline{F}\right)\right) \tag{39}$$

where $P_{ci}$ is the crossover probability of individual $i$. $P_{mi}$ is the mutation probability of individual $i$. $P_{c0}$ and $P_{m0}$ are the initial values of cross probability and variation probability. $\alpha_1$, $\alpha_2$, $\beta_1$ and $\beta_2$ are the correction factor, their values are 0.9, 1.4, 1.2, and 0.7, respectively. $f(avg)$ is the average individual fitness in current populations. $\mu$ is the difference between maximum fitness and minimum fitness. $\gamma$ is a constant value used to judge the convergence of the algorithm.

As shown in Figs. 3 and 4, this paper adopts a multipoint crossover method to implement the crossover operation and a combination of multipoint mutation and swap mutation to perform the mutation operation. The crossover and mutation mainly operate on the genes for workdays, overtime, and production priority, while the genes for product type, production month, and number of equipment remain unchanged. When individuals undergo mutation, the probabilities for multipoint mutation and swap mutation are 0.35 and 0.65, respectively. It is noteworthy that the production priority gene has a certain particularity, meaning that within the same batch of production, no two products can have the same priority. Therefore, the production priority gene only changes during the swap mutation operation.

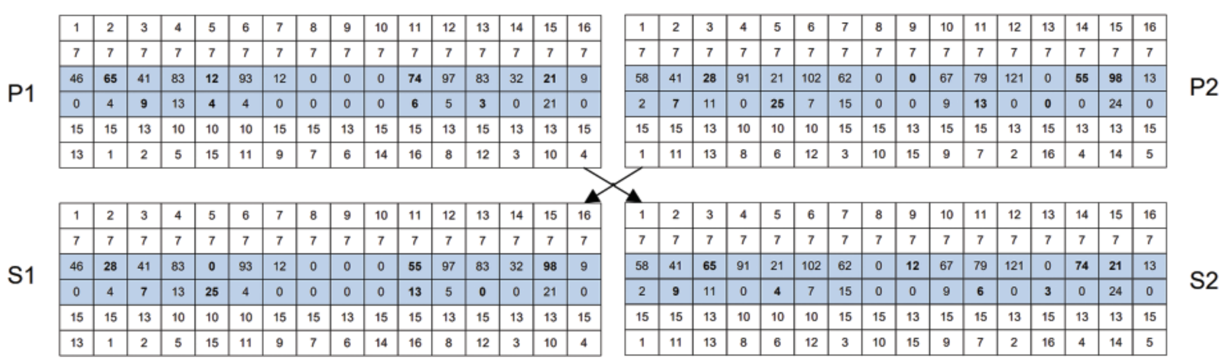


**Figure 3:** Multipoint crossover

### *3.3 Algorithm Performance Test*

In order to verify the performance of the algorithm, this paper tested five optimization algorithms—NSGA-II, particle swarm optimization, artificial protozoa optimizer, black kite algorithm, and APO-NSAGA—using the cec2020 test set and the objective functions designed in this paper. For analysis, we selected the rotated and shifted multimodal functions F2, composite functions F8, and F9, which are good representations of algorithm performance. NSGA-II and APO serve as the foundational algorithms for the design of this paper's approach; PSO is a classic heuristic algorithm with a wide range of applications and a well-established research framework; BKA is a newly proposed algorithm with excellent performance. Comparing these algorithms effectively demonstrates the performance of the APO-NSAGA. The parameter settings for the algorithms are as follows:

population size of 50, 500 iterations, dimension of 20, running on a Windows 11 64-bit system with an AMD Ryzen 9 7945HX processor and 32 GB of memory. Additionally, the initial crossover and mutation probabilities for the APO-NSAGA were set to 0.6 and 0.4, respectively.

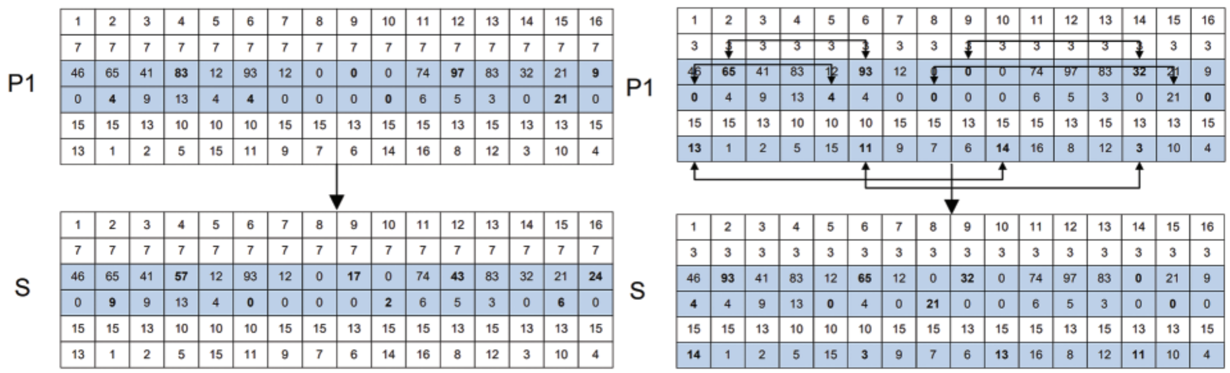


**Figure 4:** Multipoint variation and exchange variation

As shown in Fig. 5, for function F2, the APO-NSAGA algorithm exhibits strong performance in both convergence accuracy and speed, achieving the highest quality solution while balancing speed. Fig. 6 shows that for function F8, the performance of the APO-NSAGA is comparable to that of BKA. Fig. 7 indicates that for function F9, APO-NSAGA's overall performance is slightly inferior to BKA but still better than PSO, NSGA-II, and APO. Fig. 8 illustrates that for the objective function, the APO-NSAGA excels in convergence accuracy. At 20 iterations, even before the algorithm fully converged, it still outperformed the other four algorithms. Based on the above analysis, the APO-NSAGA performs well on the CEC2020 test set. Compared to some advanced heuristic algorithms, it is not inferior; each has its own strengths and weaknesses. However, in solving the master production schedule optimization problem, the APO-NSAGA demonstrates superior performance and can achieve more precise results.

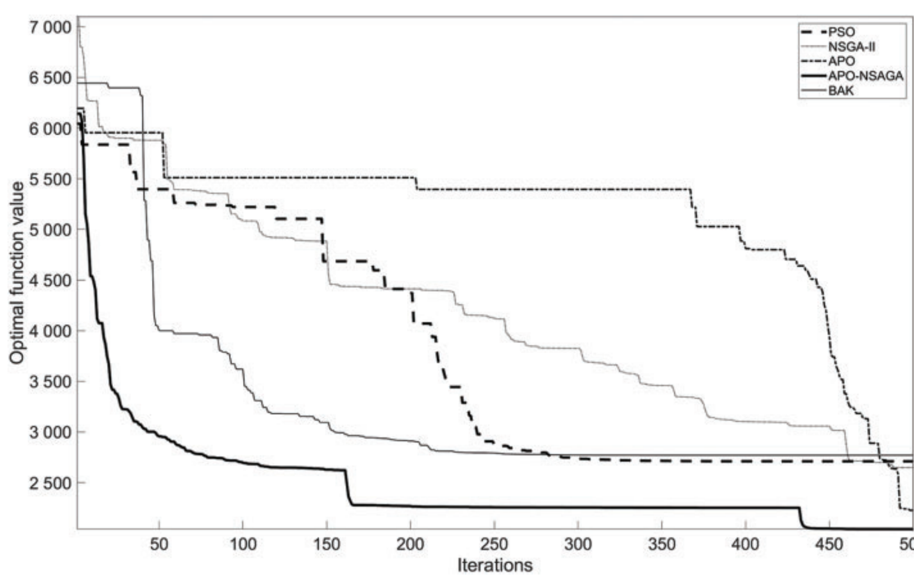


**Figure 5:** Iterative curve of each optimization algorithm under the test function $F_2$

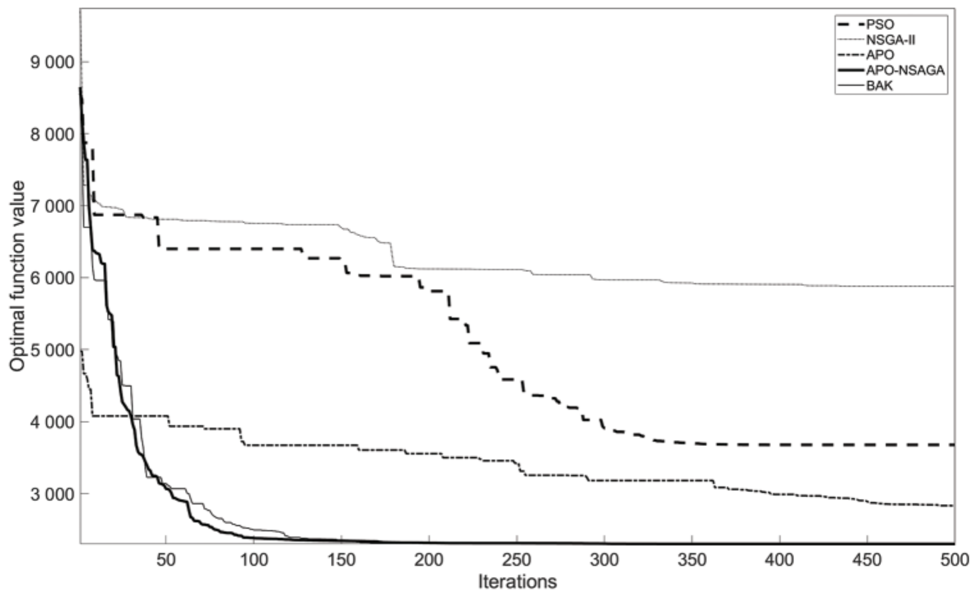


**Figure 6:** Iterative curve of each optimization algorithm under the test function $F_8$

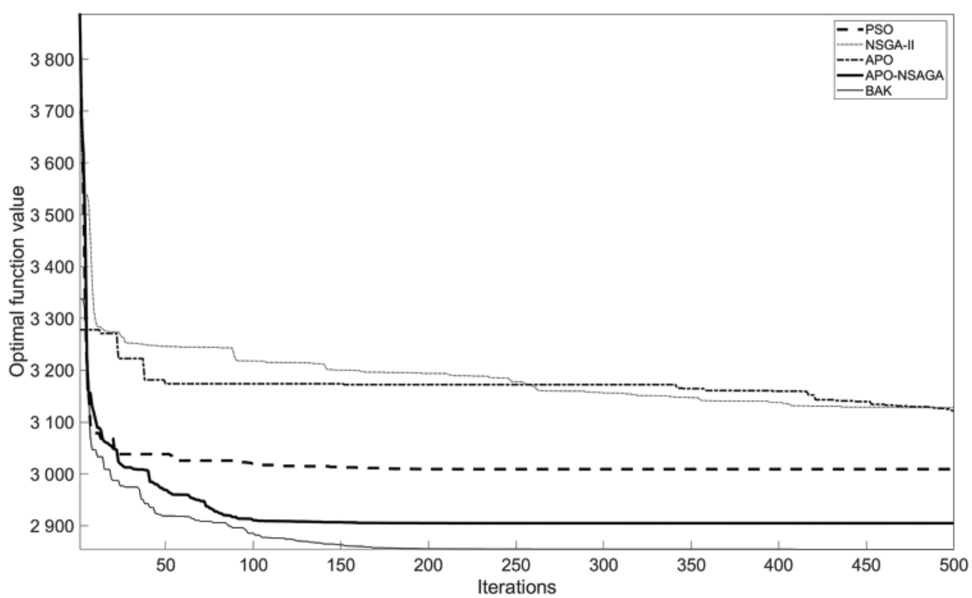


**Figure 7:** Iterative curve of each optimization algorithm under the test function $F_9$

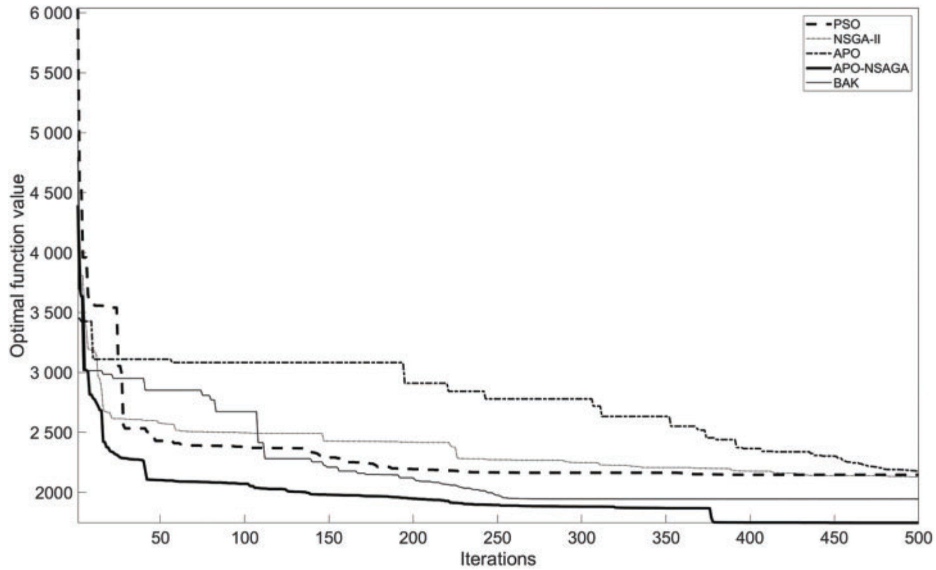


**Figure 8:** Iterative curves of each optimization algorithm under the objective function

## 4 Case Simulation

This paper takes A tobacco company as the research object and selects 16 products and 39 pieces of production equipment to formulate a master production schedule for analysis. These 16 products can be divided into 3 categories, and each category of products needs to choose the corresponding production equipment for production and processing. The specific relationship between products and equipment is shown in Table 3; the types and production capacities of each piece of equipment are shown in Table 4.

**Table 3:** The relationship between the product category and the production equipment

| Product category | Product number | Available equipment number |
|---|---|---|
| A | 1, 2, 10, 11, 13, 16 | 3, 4, 5, 6, 7, 8, 9, 10, 11, 12, 13, 14, 15, 16, 17 |
| B | 3, 8, 9, 12, 14 | 1, 2, 18, 19, 20, 21, 22, 23, 24, 25, 26, 27, 28 |
| C | 4, 5, 6, 7, 15 | 30, 31, 32, 33, 34, 35, 36, 37, 38, 39 |

**Table 4:** Equipment type and production capacity

| Equipment type | Equipment number | Productive capacity |
|---|---|---|
| AGDS | 1, 2, 3, 4, 5 | 300 cases/day |
| BVG | 6, 7, 8, 18, 19, 20, 21, 22, 23, 24, 25, 26, 27, 28 | 120 cases/day |
| DZJD | 9 | 100 cases/day |
| CPRO | 10, 11, 12 | 225 cases/day |
| CZJ | 13, 14, 15, 16, 17, 38, 39 | 150 cases/day |
| AGDX1 | 29, 30, 31, 32, 33, | 90 cases/day |
| CGDX2 | 34, 35, 36, 37 | 75 cases/day |

Based on the above data, the APO-NSAGA was used to solve the production scheduling problem, selecting typical products 5, 8, 11, 13, and 14 for result analysis. The parameter settings for the algorithms are as follows: population size of 200, 600 iterations, initial crossover and mutation probabilities of 0.6 and 0.4, running on a Windows 11 64-bit system with an AMD Ryzen 9 7945HX processor and 32 GB of memory. By formulating a master production schedule, detailed analyses of the data before and after optimization were conducted. It should be noted that the master production schedule started in February and ended in January of the following year.

### *4.1 Output Analysis*

As shown in Fig. 9, the monthly output variance of product 5 decreased from $6.29 \times 10^7$ to $2.81 \times 10^7$ after optimization, a reduction of 55.32%. The monthly output variance of product 8 decreased from $1.39 \times 10^6$ to $1.29 \times 10^6$ after optimization, a reduction of 7.19%. The monthly output variance of product 13 decreased from $2.17 \times 10^7$ to $1.72 \times 10^7$ after optimization, a reduction of 20.74%. The monthly output variance of product 14 decreased from $2.56 \times 10^4$ to $1.53 \times 10^4$ after optimization, a reduction of 40.23%. Among the five typical products, products 5 and 13 are particularly representative. For product 5, the maximum monthly production before optimization was 20,520 boxes, occurring in August, while after optimization, the maximum monthly production was reduced to 15,600 boxes in November, a decrease of 23.98%. For product 13, the maximum monthly production before optimization was 13,200 boxes in May, and after optimization, it dropped to 11,935 boxes in January of the following year, a reduction of 9.6%. Additionally, product 5 experienced the greatest fluctuations in production during July, August, and September, with a production increase of 185% from July to August, while production in September dropped to zero. Product 13 showed the most significant fluctuations in September, October, and November, with its production increasing from zero in September to 12,770 boxes in October, followed by a steep decline of 64.76% in November. After the master production schedule optimization, at the same time points, the production increase for product 5 was reduced by 76.7%, and for product 13, the production increase dropped from the original 12,770 boxes to 9675 boxes, representing a 24.24% reduction. The production decrease for product 5 was reduced from 100% to 26.4%, while for product 13, the production drop was reduced from 64.76% to 37.15%.

As shown in Fig. 10, the annual average output variance of category A products decreased from $2.14 \times 10^8$ to $1.74 \times 10^8$ after optimization, a reduction of 18.97%. The annual average output variance of category B products decreased from $6.92 \times 10^7$ to $4.32 \times 10^7$ after optimization, a reduction of 37.59%. The annual average output variance of category C products decreased from $1.83 \times 10^7$ to $1.51 \times 10^7$ after optimization, a reduction of 17.49%. Simultaneously, the optimized master production schedule reduced the total production cost of Company A by 7.56%. In addition, before the optimization of the master production schedule, the highest monthly capacity utilization rates for products A, B, and C reached 97.86%, 99.46%, and 99.01%, respectively, with variances in monthly capacity utilization rates of 0.064, 0.027, and 0.043, respectively. After the optimization, the highest monthly capacity utilization rates for products A, B, and C dropped to 90.96%, 96.93%, and 93.67%, representing decreases of 7.05%, 2.54%, and 5.39%, respectively. The variances in monthly capacity utilization rates also decreased to 0.046, 0.022, and 0.034, representing reductions of 28.13%, 18.52%, and 20.93%, respectively.

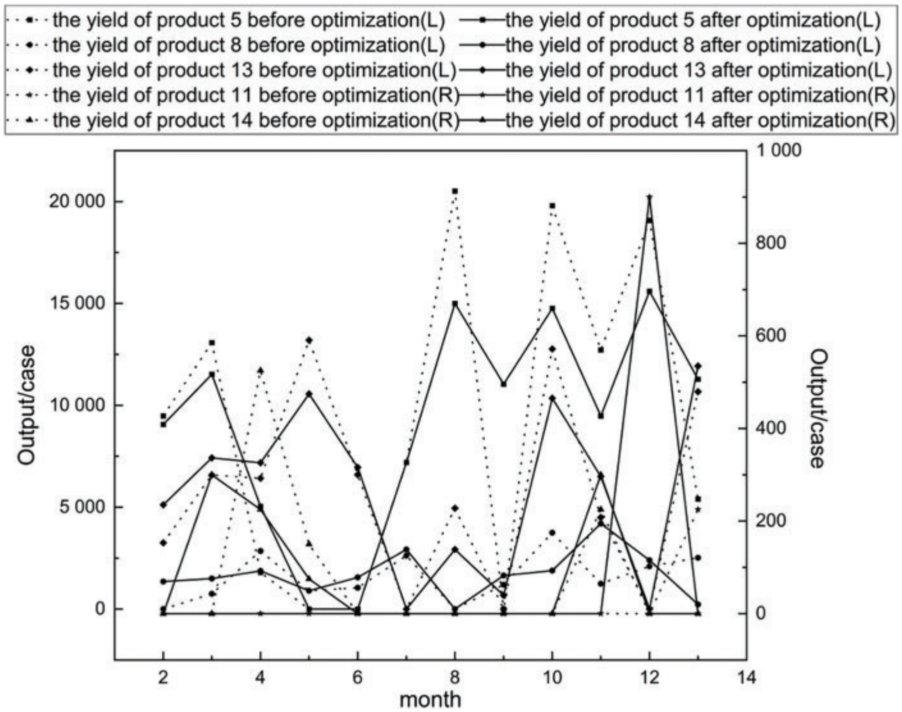


**Figure 9:** The monthly output of typical products before and after the optimization of master production schedule

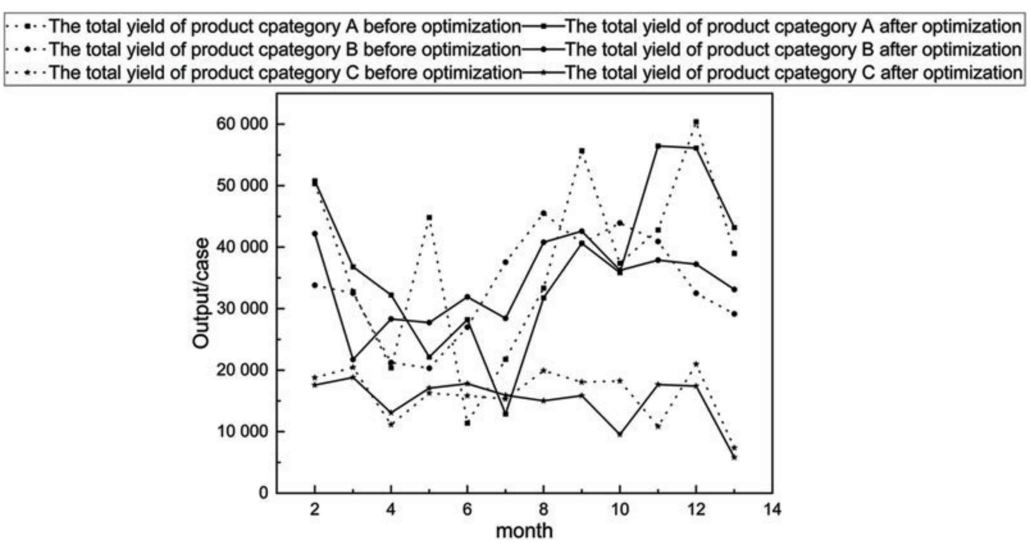


**Figure 10:** The monthly output of various products before and after the optimization of master production schedule

Based on the above analysis, it can be concluded that the optimized master production schedule effectively balances the monthly production of each product, reduces fluctuations in monthly production, and balances the capacity utilization rates for various products. While reducing the peak capacity utilization rates, the optimization improves the peak capacity utilization, thereby increasing the tolerance of the enterprise's production system.

### 4.2 *Analysis of Sales Volume and Demand*

As shown in Fig. 11, before the optimization, there were six months (February, March, September, October, November, and December) where the available product volume was less than the actual demand, resulting in stockouts and an inability to meet market demand. Specifically, product 5 experienced a stockout in September with a shortfall of 878 boxes, accounting for 8.13% of the actual demand for that month; product 8 had consistent stockouts in both February and March, with shortfalls of 1000 boxes and 465 boxes, representing 100% and 38.27% of the actual demand for those months, respectively; product 11 had a stockout in November with a shortfall of 394 boxes, accounting for 63.65% of the actual demand; product 13 experienced a stockout in February with a shortfall of 860 boxes, representing 20.90% of the actual demand; and product 14 had a stockout in March with a shortfall of 173 boxes, representing 100% of the actual demand. However, as shown in Fig. 12, after optimization, the available volume of products in each month exceeded the actual demand, fully meeting market requirements.

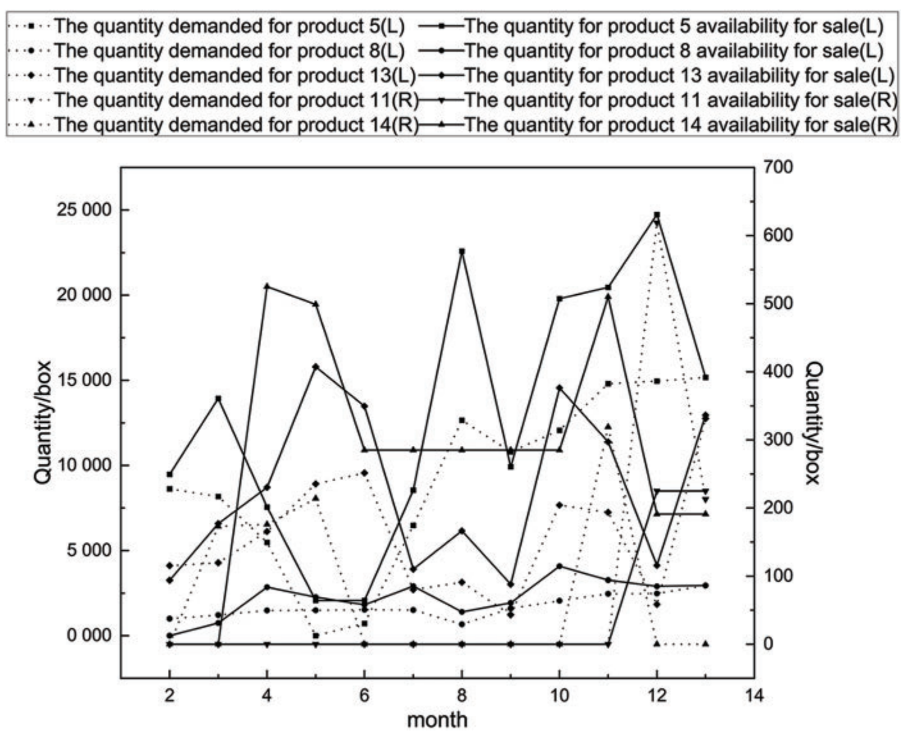


**Figure 11:** The monthly available for sale and demand before the optimization of master production schedule

From the above analysis, it can be concluded that the optimized master production schedule effectively plans the monthly production volume of each product, reasonably addresses market demand, improves the company's order fulfillment rate and market satisfaction, and further promotes the company's development.

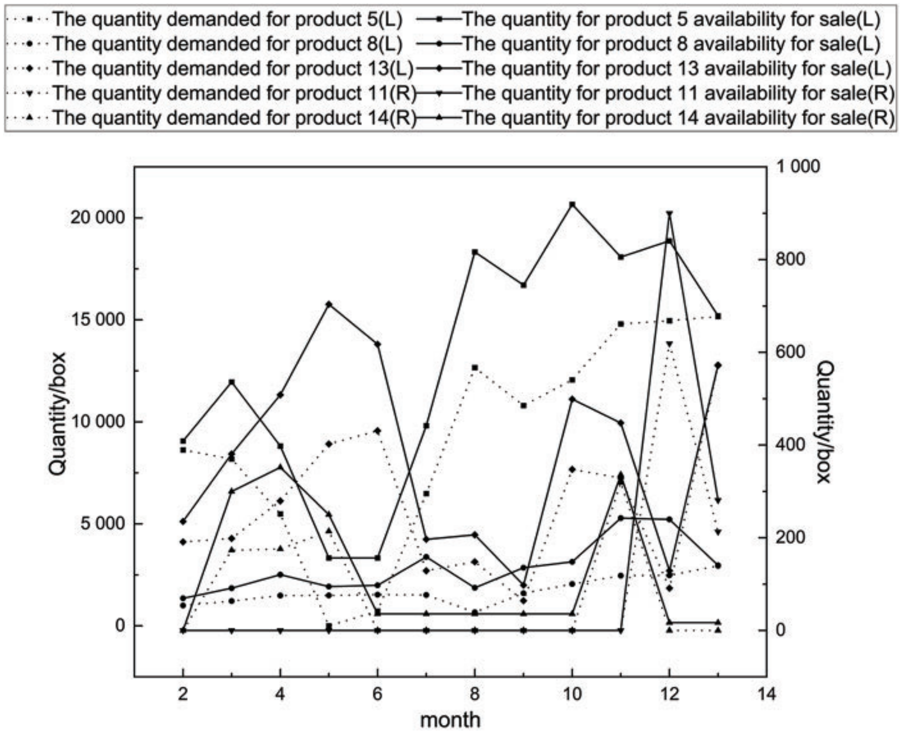


**Figure 12:** The monthly available for sale and demand after the optimization of master production schedule

### *4.3 Inventory Analysis*

Fig. 13 displays the end-of-month inventory for typical products. Consequently, the maximum inventory across all 16 products decreased from 83,344 cases to 51,880 cases, a reduction of 37.75%. The average inventory decreased from 48,674 cases to 39,088 cases, a reduction of 19.69%. The year-end remaining inventory decreased from 14,030 cases to 486 cases, a reduction of 96.53%.

Fig. 14 shows the changes in the stock-to-sales ratio for five typical products. The stock-to-sales ratio refers to the ratio of the ending inventory for the current month to the forecasted demand for the following month, reflecting the relationship between inventory levels and sales demand. It provides a reasonable evaluation and description of the company's inventory situation. As shown in the figure, the maximum stock-to-sales ratio for product 5 decreased from 89.0 to 21.3 after optimization, a reduction of 76.07%, and the variance decreased from 600.2 to 47.5, a reduction of 92.09%. For product 8, the maximum stock-to-sales ratio decreased from 64.7 to 48.2, a reduction of 25.50%, and the variance decreased from 340.7 to 177.7, a reduction of 47.84%. For product 13, the maximum stock-to-sales ratio decreased from 69.4 to 48.6, a reduction of 29.97%, and the variance decreased from 681.5 to 260.1, a reduction of 61.83%. For product 14, the maximum stock-to-sales ratio decreased from 50.5 to 25.4, a reduction of 49.70%, and the variance decreased from 342.5 to 116.7, a reduction of 65.93%. Additionally, the average stock-to-sales ratio for all 16 products decreased from 26.45 to 13.50, a reduction of 48.96%, and the variance decreased from 7104.6 to 177.5, a reduction of 97.50%.

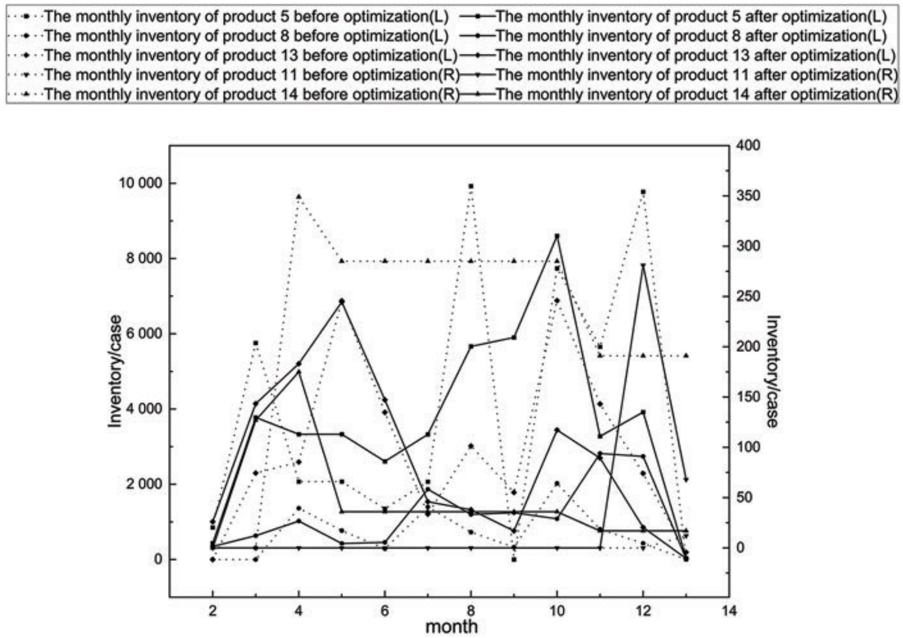


**Figure 13:** The amount of inventory at the end of each month before and after the optimization of master production schedule

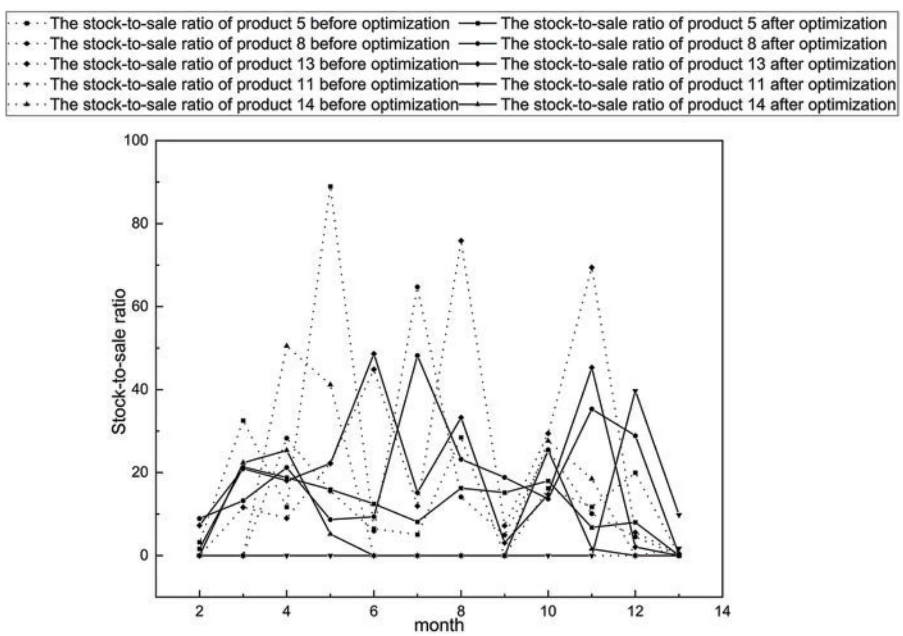


**Figure 14:** The stock-to-use ratio of each month before and after the optimization of master production schedule

Inventory turnover rate reflects the speed at which a company's inventory is cycled, with a higher turnover rate indicating faster inventory turnover and better product sales performance. A good inventory turnover rate helps a company quickly recover its working capital, promoting better development. As shown in Fig. 15, the average monthly inventory turnover rate increased from 1.84 to 2.26, an increase of 22.83%; the maximum inventory turnover rate increased from 3.2 to 5.7, an increase of 78.13%; and the minimum inventory turnover rate increased from 1.2 to 1.6, an increase of 33.33%. Meanwhile, the inventory turnover days decreased from 16.3 days to 13.27 days, a reduction of 18.59%; the maximum inventory turnover days decreased from 25.8 days to 17.8 days, a reduction of 31.01%; and the minimum inventory turnover days decreased from 9.3 days to 5.3 days, a reduction of 43.01%.

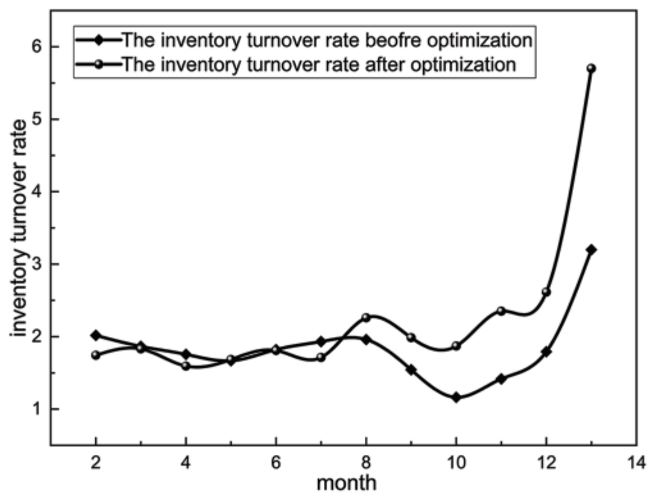


**Figure 15:** The inventory turnover of each month before and after the optimization of master production schedule

In summary, the optimized master production schedule effectively reduces the company's maximum inventory level and year-end inventory, decreases stagnant inventory, optimizes the stock-to-sales ratio of various products, reduces fluctuations in the stock-to-sales ratio, and improves the rationality of the company's inventory structure and its ability to withstand market demand fluctuations. Additionally, it increases the inventory turnover rate, thereby improving the company's cash flow and promoting further development.

## 5 Conclusion and Future Work

This paper explores the optimization problem of the master production schedule for fast-moving consumer goods enterprises. Based on the constructed optimization model, an improved APO-NSAGA was designed to solve the model. Finally, through case simulation, the following conclusions were drawn:

(1) The optimized master production schedule can effectively balance the monthly output of various products, reducing output fluctuations and addressing the common issue of uneven capacity utilization in FMCG enterprises.

(2) The optimized master production schedule can effectively improve the service level of enterprises, enabling them to complete production tasks on time in a "pull" mode and meet market demand.

(3) The optimized master production schedule can effectively reduce the inventory level of enterprises, improve inventory turnover, and free up more working capital for business operations.

This study on the optimization of the master production schedule did not overly consider the supply of raw and auxiliary materials. The uncertainties caused by suppliers and transportation leading to shortages of raw and auxiliary materials in actual production processes have not been specifically studied and will be discussed further.

**Acknowledgement:** The authors are very grateful to Rengwang Li, for he provided the opportunity to carry out this study. The authors would also like to express their sincere appreciation to all those who have participated in the research of the composite scheduling project and, therefore, contributed to some extent to the elaboration of this paper.

**Funding Statement:** The authors received no specific funding for this study.

**Author Contributions:** Fanghua Ning conceived of the presented idea. Yutao Jin developed the theory and performed the computations. Panlong Zhang and Xiangyu Yang verified the analytical methods. All authors reviewed the results and approved the final version of the manuscript.

**Availability of Data and Materials:** Data available on request from the authors.

**Ethics Approval:** Not applicable for studies not involving humans or animals.

**Conflicts of Interest:** The authors declare no conflicts of interest to report regarding the present study.

**References**

1. Chen YJ. Analysis of the status quo of China's fast consumer goods industry and suggestion for improvement. North Econ. 2018;405(8):28–9 (In Chinese). doi:10.3969/j.issn.1005-913X.2018.08.012.
2. Zhou J. Enterprise inventory management problems and their improvement strategies. Enterp Reform Manag. 2022;438(13):85–7 (In Chinese). doi:10.13768/j.cnki.cn11-3793/f.2022.0703.
3. Framinan JM, Guerrero F, Gonzalez PP, Toscano S. Matching inventory and demand in a fast moving consumer goods company: a decision support system. Comput Ind Eng. 2024;194:110377. doi:10.1016/j.cie.2024.110377.
4. Peng YF, Lu DD. Fuzzy hierarchial production planning model of multi-product discrete manufacturing with uncertain demand. Mod Manuf Eng. 2015;410(8):27–34 (In Chinese). doi:10.16731/j.cnki.1671-3133.2015.08.028.
5. Wang Y, Shi Q, Li L, Li F, Xia W. Spare parts supply network optimization with uncertain distributed lead time and demands. Rev Int Métodos Numér Cálc Diseño Ing. 2021;37(1):1. doi:10.23967/j.rimni.2020.11.002.
6. Li C, Li B, Wang Y, Bai C, Zhang X. Data mining based production planning and scheduling algorithm for power metering equipment. Manuf Autom. 2023;45(4):88–91 (In Chinese). doi:10.3969/j.issn.1009-0134.2023.04.019.
7. Liu YF, Zhang QS. Multi-variety product planning model for manufacturing enterprises with multiple uncertainties in demand. J Liaoning Tech Univ. 2020;39(1):93–8 (In Chinese). doi:10.11956/j.issn.1008-0562.2020.01.015.
8. Jing Y, Li Q. Multi-objective planning model and algorithm for coordinative production considering individual interests in the multi-factory environment. Oper Res Manage Sci. 2020;29(2):212–8 (In Chinese). doi:10.12005/orms.2020.0054.
9. Masruroh NA, Putra RKE, Mulyani YP, Rifai AP. Strategic insights into recovery from supply chain disruption: a multi-period production planning model. J Oper Res Soc. 2022;74(7):1–25. doi:10.1080/01605682.2022.2115414.

10. Yazd SANN, Salamirad A, Kheybari S, Ishizaka A. An efficiency-based aggregate production planning model for multi-line manufacturing systems. Oper Manage Res. 2023;16(4):1–17. doi:10.1007/s12063-023-00381-0.
11. Razm S, Brahimi N, Hammami R, Dolgui A. A production planning model for biorefineries with biomass perishability and biofuel transformation. Int J Prod Econ. 2023;258(7):108773. doi:10.1016/j.ijpe.2023.108773.
12. Marfuah U, Mutmainah, Panudju AT, Mansyuri U. Dynamic programming approach in aggregate production planning model under uncertainty. Int J Adv Comput Sci Appl. 2023;14(3):0140321. doi:10.14569/IJACSA.2023.0140321.
13. Bazo do Nascimento M, Scarpin C. No-wait open shop with worker flexibility. Rev Int Métodos Numér Cálc Diseño Ing. 2021;37(2):26. doi:10.23967/j.rimni.2021.04.005.
14. Deng H, Shi Q, Wang Y. Joint optimization of condition-based maintenance and inventory ordering based on status monitoring for multi-unit system. Rev Int Métodos Numér Cálc Diseño Ing. 2021;37(4):45. doi:10.23967/j.rimni.2021.10.005.
15. Chaudhry I, Elbadawi I, Rafique A, Boudjemline A, Boujelbene M, Usman M, et al. Minimization of completion time variance in flowshops using genetic algorithms. Rev Int Métodos Numér Cálc Diseño Ing. 2022;38(2):22. doi:10.23967/j.rimni.2022.05.002.
16. Ferreira J, Steiner M. A complexity task of optimization in logistic distribution: a new approach to the green multi-objective vehicle routing problem. Rev Int Métodos Numér Cálc Diseño Ing. 2022;38(1):3. doi:10.23967/j.rimni.2022.01.001.
17. Wang CC, Yang CL, Zhang T. Order planning with an outsourcing strategy for a make-to-order make-to-stock production system using particle swarm optimization with a self-adaptive genetic operator. Comput Ind Eng. 2023;182(1):109420. doi:10.1016/j.cie.2023.109420.
18. Guzman E, Poler R, Andres B. A matheuristic approach combining genetic algorithm and mixed integer linear programming model for production and distribution planning in the supply chain. Adv Prod Eng Manage. 2023;18(1):19–31. doi:10.14743/apem2023.1.454.
19. Bojic S, Maslarić M, Mirčetić D, Nikolicic S. Simulation and Genetic Algorithm-based approach for multi-objective optimization of production planning: a case study in industry. Adv Prod Eng Manage. 2023;18(2):250–62. doi:10.14743/apem2023.2.471.
20. Lin FY, Wen YS. Deep neural network accelerated-group African vulture optimization algorithm for unit commitment considering uncertain wind power. Appl Soft Comput. 2024;162:111845. doi:10.1016/j.asoc.2024.111845.
21. Wang J, Wang WC, Hu XX, Qin L. Black-winged kite algorithm: a nature-inspired meta-heuristic for solving benchmark functions and engineering problems. Artif Intell Rev. 2024;57(4):98. doi:10.1007/s1046-10723-4.
22. Wang WC, Tian WC, Xu DM, Zang HF. Arctic puffin optimization: a bio-inspired metaheuristic algorithm for solving engineering design optimization. Adv Eng Softw. 2024;195:103694. doi:10.1016/j.advengsoft.2024.103694.
23. Wang XP, Snášel V, Mirjalili S, Pan JS. Artificial Protozoa Optimizer (APO): a novel bio-inspired metaheuristic algorithm for engineering optimization. Knowl-Based Syst. 2024;295(8):111737. doi:10.1016/j.knosys.2024.111737.
24. Trost M, Claus T, Herrmann F. Master production scheduling with consideration of utilization-dependent exhaustion and capacity load. Sustainability. 2023;15(8):6816. doi:10.3390/su15086816.
25. Shekhar DRT, Mahajan A, Hemachandra N. Mathematical modeling of master production schedule with campaign planning constraints. In: 2021 IEEE Industrial Engineering and Engineering Management (IEEM), 2021; Singapore; p. 964–68. doi:10.1109/IEEM50564.2021.9672996.
26. Abad P. Optimal pricing and lot-sizing under conditions of perishability, finite production and partial backordering and lost sale. Eur J Oper Res. 2003;144(3):677–85. doi:10.1016/S0377-2217(02)00159-5.

27. Eisa A, AbouHawa M, Fattouh M. Multi-objective optimization of HS-WEDM for hole cutting in thin-walled CFRP composites using COCOSO and genetic algorithms. J King Saud Univ-Eng Sci. 2024. doi:10.1016/j.jksues.2024.06.001.
28. Drissi El-Bouzaidi M, El Bardouni T, Chham E, El Hajjaji O, Nouayti A, Idrissi A, et al. Unfolding of the neutron spectrum in a nuclear reactor using genetic algorithms method. Nucl Eng Des. 2024;422:113156. doi:10.1016/j.nucengdes.2024.113156.